Bond-Counting Rule for Carbon and its Application to the Roughness of Diamond (001)

H. X. Yang, L. F. Xu, Z. Fang, and C. Z. Gu

Beijing National Laboratory for Condensed Matter Physics, Institute of Physics, Chinese Academy of Sciences, P.O. Box 603, Beijing 100080, China

S. B. Zhang

Department of Physics, Applied Physics, and Astronomy, Rensselaer Polytechnic Institute, Troy, New York 12180, USA

(Received 26 March 2007; published 14 January 2008)

Despite that carbon is tetravalent identical to silicon, first-principles calculations reveal that stable step structures on diamond (001) are entirely different from those on silicon. Moreover, pristine Si(001) is flat; pristine diamond (001) could be rough due to negative step formation energies. A generic bond-counting rule is established, which should apply to most carbon structures where sp^2 and sp^3 hybrids coexist: e.g., it provides a qualitative account of the step energy order without detailed calculation. Our findings agree with experimental observations.

DOI: 10.1103/PhysRevLett.100.026101 PACS numbers: 68.35.B−, 68.35.Ct, 68.35.Md, 81.05.Uw

Diamond is attractive because of its unique and exceptional combination of electrical, optical, thermal, and chemical properties [1–3]. It has been extensively studied for applications such as field effect transistors and in high power electronics, as well as super hard coatings for cutting tools. In developing such applications, it is indispensable that we know the surface properties. For a long time, it has been generally accepted that a pristine diamond (001) surface is flat, with a symmetric dimer (2×1)-reconstruction [4]; steps are less stable because they could lead to an excess of strains and/or extra surface dangling bonds. This is indeed the case for the (001) surface of silicon, which has the same bulk crystal structure as diamond. According to the calculation for silicon, the most stable step structure, which does not have either extra dangling bonds or large strains, is still about 0.01 eV per unit step length higher in energy than the flat surface [5].

Carbon is, however, fundamentally different from silicon, as carbon has a much shorter bond length and hence a much stronger tendency to form π bond [4], leading to a rich variety of organic chemistry as well as graphite/fullerene chemistry, virtually none existing in Si. Indeed, a recent calculation showed marked differences between diamond and silicon: the high-miller index {311} diamond surfaces are stable [6], and due to this the {001} faces may not exist on the surfaces of diamond nanoparticles [7]. By examining steps on the diamond (001) surfaces, here we establish a simple generic bond-counting (BC) rule, parallel to the electron-counting rule for binary semiconductor surfaces [8] and metal adsorbates [9], to apply to carbon systems where sp^2 and sp^3 configurations coexist. The rule has three elementary components: (i) A π bond is far more stable than two dangling bonds (DB), each with one electron; (ii) one only has to examine the bond length to determine if a bond is a single σ or a double $(\sigma + \pi)$ bond; and (iii) each carbon atom should be fourfold coordinated if also taking into account all the π bonds at the surfaces.

In particular, we have systematically studied the stabilities of both single- and double-layer steps on diamond (001) surfaces. The formation energies for a large number of different atomic configurations, with various types of reconstructions at the step edges, were calculated by using first-principles density functional theory. Aside from establishing the genetic bond-counting rule, we also found that steps on the pristine diamond (001) surfaces are energetically more favorable than the flat surfaces. In other words, flat surfaces have the tendency to transform into rough surfaces. The application of the BC rule further allows for a qualitative account of the energy order of the steps without any detailed calculations. It shows that, while π bonding is essential to the stabilization of the low-energy structures, the primary reason for the negative step energies is the reduction of the strained σ bonds at the step edges. Our prediction agrees with recent STM experiments [10].

We carried out the calculations by using the Vienna *ab initio* simulation package (VASP) [11–13], in which the electron-core interactions were described by the Vanderbilt ultrasoft pseudopotential [14], and the exchange correlation energy was obtained within the generalized gradient approximation [15]. A plane wave basis set was used to expand the Kohn-Sham orbitals with a 350-eV kinetic energy cutoff. The calculated lattice constant of diamond 3.574 Å is only 0.2% larger than the experimental value of 3.567 Å. To mimic the (001) surfaces, a supercell approximation was used in which each slab is separated from the neighboring slabs by at least 10 Å of vacuum. Hydrogen atoms were used to passivate bottom surfaces. The Monkhorst-Pack scheme [16] was used for the Brillouin zone integration, and we have tested that a $4 \times 4 \times 1$ k-point mesh is sufficient to ensure a good convergence in the total energy differences. In the energy minimization, we have allowed for the atoms to fully relax according to the atomic forces, except for those at the bottom two layers, which are fixed at their respective positions of the (2×1) surface. The energy convergence

for the structural optimization is better than 0.5 meV per atom.

Similar to silicon [5], the large number of single-layer (S) and double-layer (D) step structures on diamond (001) surfaces can be classified into four distinct groups: S_A, S_B, D_A, and D_B, where subscripts A and B denote the steps with their edges parallel and perpendicular to the dimer *rows* on the upper terrace, respectively. Figures 1(a)–1(d) show, in a top view, the representative nonbonded structures of the four basic types of steps. In addition, Fig. 1(e) shows a mini-terrace (mt) D_A structure to be discussed below.

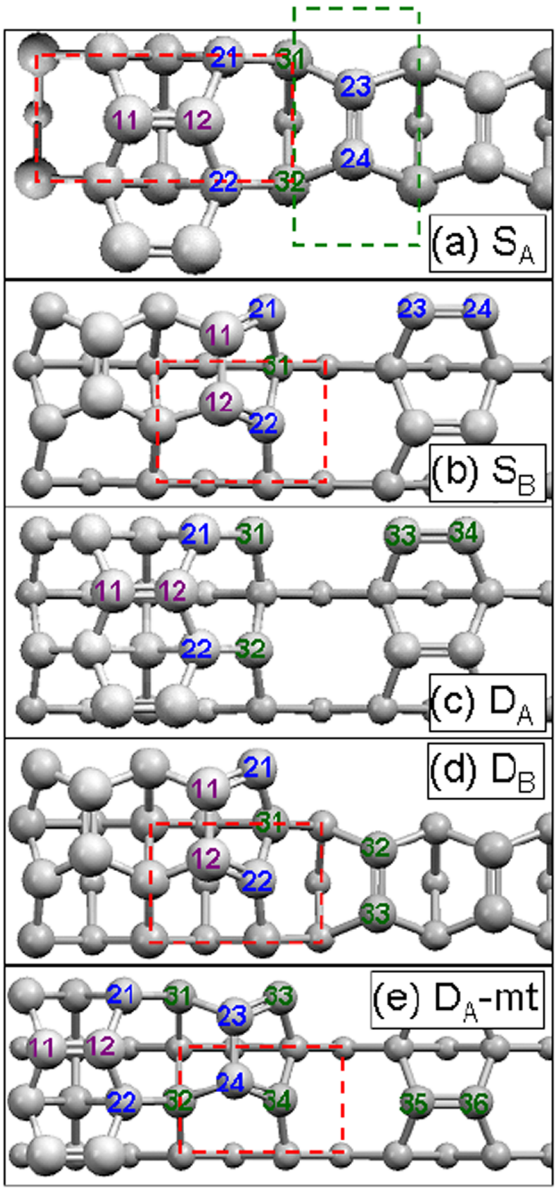

FIG. 1 (color online). Top view of the nonbonded (a) S_A, (b) S_B, (c) D_A, (d) D_B, and (e) mini-terrace D_A steps. A convention of double-digits labeling of the atoms is adopted here, in which the first number indicates the layer at which the atom resides, and the second number numerates the atoms in that layer. Bonds with a length of 1.50 ± 0.02 Å or longer are shown with single lines, whereas bonds with a length of 1.38 ± 0.01 Å are shown with double lines.

To ensure an accurate determination of the step energies, the calculations were carried out in steps. In step I, we calculated the relative energy difference between the single- and double-layer steps by using high-Miller index vicinal surfaces. For example, the $(\bar{1}, 1, 13)$ and $(1, 1, 13)$ surfaces, both with a tilt angle of 6.1° from the (001) surface, were used to calculate the energies of the double-layer D_A and D_B steps, relative to that of a single-layer S_A and S_B pair. This gives

$$\lambda(D_A) - [\lambda(S_A) + \lambda(S_B)] = 1.11 \text{ eV}/a_s, \quad (1)$$

and

$$\lambda(D_B) - [\lambda(S_A) + \lambda(S_B)] = 0.08 \text{ eV}/a_s, \quad (2)$$

where λ is the energy difference (per unit step length) between the single- and double-layer steps and $a_s = 2.53$ Å is the surface lattice constant. The reason for calculating the relative energies is to preserve the unit cell dimensions and the number of atoms, so the computational errors can be minimized by a cancellation of errors [5]. In step II, the formation energies of the S_A and D_B steps, $\lambda(S_A)$ and $\lambda(D_B)$, were individually calculated by using a 2×7 and a 8×2 surface unit cell, respectively; each contains a trench structure terminated at both ends by the same steps. In other words, each supercell here contains two identical steps.

In step III, the energies of the S_A and D_B steps were compared with that of a flat (2×1) surface to obtain the absolute step formation energies. Note that extra caution is required here because it is no longer possible to compare systems with the same dimensions and the same number of atoms. In the current case, we used a carbon atomic reservoir of chemical potential μ_c. The absolute value of the μ_c can be calculated by using an accurate and physically inspired step-flow growth method [17,18]. We have changed the slab thickness, cell dimension, and k-point sampling in the calculation to make sure that the errors in step III are less than 20 meV per unit step length.

Figure 2 summarizes the calculated results for the step formation energies in four panels: the nonbonded S_A, S_B, D_A, and D_B, the rebonded S_B, D_A, and D_B, and a new mini-terrace D_A structure [Fig. 1(e)]. The results for diamond are given to the lefts, whereas those for silicon are given to the rights, for comparison. We see from Fig. 2 that step stabilities on diamond (001) surfaces are completely different from those on silicon (001) surfaces. These include: (i) except for the S_A step, none of the stable structures of silicon are stable in diamond; the formation energies of these rebonded structures of roughly 1 eV/a_s are in fact exceedingly high. (ii) Noticeably, step formation energies of Si(001) are all positive [5,19,20] with that of S_A being the lowest, whereas those of diamond are all negative with

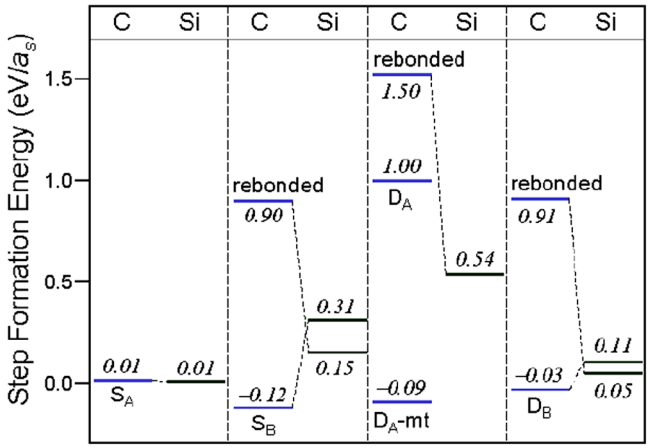

FIG. 2 (color online). Calculated step formation energies with respect to that of the flat (001) − (2 × 1) surface. In each panel, lines to the lefts are for diamond, whereas lines to the rights are for silicon. Data for silicon are taken from Refs. [5,20].

S_A being the only exception and hence least stable. In the case of the S_B step for diamond, the formation energy is rather significant, more than 0.1 eV/a_s negative. (iii) While the rebonded structures are energetically favored in silicon, it is the nonbonded ones that in general have lower energies in diamond.

These qualitative differences between diamond and silicon can be traced back to their different chemistry: there is no p state in the carbon core. The carbon $2p$ valence states are thus more localized than the corresponding silicon $3p$ valence states, resulting in a much shorter bond length and a much stronger tendency of π bonding. The lack of stable rebonded structures is a direct result of the shorter bond length, which makes the rebonding energetically costly. One can determine which bond is a single σ and which bond is a double ($\sigma + \pi$) simply by examining their bond lengths: the length of a single bond is 1.50 ± 0.02 Å or longer; the length of a double bond is 1.38 ± 0.01 Å. This way, one can easily tell whether an atom at the step edge is threefold coordinated with a dangling bond or fourfold coordinated without any DB. Detailed atomic and electronic structure analysis supports such a simple rule of thumb without any exception.

For instance, atom 12 in Fig. 1(a) is fourfold coordinated, because it shares a double bond with atom 11. As such, there is no DB, and this is the most stable S_A step. In Fig. 1(b), atoms 11, 12, 21, and 22 are all fourfold coordinated, because double bonds exist between atoms 11 and 21, and separately between atoms 12 and 22. There is no DB, and hence this is the most sable S_B step. In Fig. 1(c), atom 12 shares a double bond with atom 11, but the threefold coordinated atom 31 (and 32), in the third layer from the top surface, still has a DB. This leaves the D_A structure relatively unstable. In Fig. 1(d), atoms 11, 12, 21, and 22 are all fourfold coordinated, as each shares a double bond with another. There is no DB, and hence this is the most stable D_B step. In other words, a simple bond-counting rule, as outlined earlier, works perfectly here, at least to the first order.

The energy penalty for the DBs in the D_A step structure is relatively large, roughly 1 eV/a_s (cf. Fig. 2). This is consistent with the strength of $\frac{1}{2}$ of the carbon-carbon π bond of 0.9 eV. This value was calculated by using the theoretical cohesive energy of carbon of 10.15 eV [21] and the (110) surface energy of 3.26 eV [21], assuming that no strained σ bond exists on the (110) surface. To search for a lower-energy D_A step structure without the DBs, we have applied the BC rule; it leads us to a new mini-terrace structure shown in Fig. 1(e). Here, atoms 23, 24, 33, and 34 at the lower terrace are all fourfold coordinated with a double bond between atoms 23 and 33, and separately between atoms 24 and 34. As expected, the elimination of the DBs from the D_A step yields significantly lower, and even negative, formation energy of -0.092 eV/a_s. We note that the mt-D_A and the low-energy S_B and D_B steps share a common local structure that has been proposed previously for stable diamond {311} surfaces.

One can use the BC rule, coupled with the concept of surface structural motifs [22], to further understand, to a second-order approximation, why the steps, other than the S_A, should have lower energy than the flat surface, without any sophisticated calculations. There are only three important surface motifs in Fig. 1:

Motif 1 [e.g., atom 11 or 12 in S_A, Fig. 1(a)]: It has two normal σ bonds, one strained σ bond ($\bar{\sigma}$) due to the dimerzation of the surface that brings 2 second-nearest neighbor C atoms to first-nearest-neighbor, and one π bond on top of the $\bar{\sigma}$ bond.

Motif 2 [e.g., atom 11 or 12 in S_B, Fig. 1(b)]: It has two σ, one $\bar{\sigma}$, and one π bond. The difference between motifs 2 and 1 is that here the π bond is at a different location.

Motif 3 (e.g., atom 21 or 22 in S_B): It has three σ and one π bond, but without any strained $\bar{\sigma}$ bond.

Note that in a covalent system, two atoms share one bond. To avoid double counting in the energy partition, therefore, all the numbers above should be multiplied by a factor of $\frac{1}{2}$. Thus, on flat (2 × 1) where every surface atom is a motif 1, each should have (σ, $0.5\bar{\sigma}$, 0.5π) bonds. For the S_A step, each step atom is a motif 1, too, same as on the (2 × 1) surface. This explains why the energy of the S_A step is so similar to that of the flat surface. On the S_B step, on the other hand, there are two types of carbon atoms, motifs 1 and 2, of equal number. Thus, on average, each step atom has $\frac{1}{2}[(\sigma, 0.5\bar{\sigma}, 0.5\pi) + (1.5\sigma, 0.5\pi)] = (1.25\sigma, 0.25\bar{\sigma}, 0.5\pi)$ bonds. The same is true for the D_B and mini-terrace D_A steps. In other words, these steps all have $\frac{1}{4}$ less strained σ bond per unit length than the flat surfaces. From the calculated surface energy difference between the (110) surface, where a π bond exists but not the strained σ bond, and the (001) surface, where a π bond coexists with a strained σ bond [21], we have estimated

that the strain on the σ bond causes 1.18 eV/bond. A $\frac{1}{4}$ of it would be 0.29 eV to lower the S_B, D_A, and D_B step energies with respect to that of the flat (2×1) surface. The differences between our simple estimate (0.3 eV) and the actual calculated numbers in Fig. 2 ($\sim$0.1 eV) may be attributed to the strain effects associated with the assembly of the motifs into actual structures, which have not been taken into account in our model.

Natural single crystal diamond (001) has been studied by using the STM [10]. Their results support our notion that the surface is rough, instead of being flat, and that all the four types of step structures are present. This is in contrast to Si in which, according to Fig. 2, the D_A step should be absent. Note that the preparation of an atomically flat surface requires hydrogen plasma. A clean surface was obtained only after dehydrogenation at 1100 °C, which automatically roughens. In contrast, clean silicon (001) will not roughen until 1350 K (or 1077 °C) [23]. Irrespective of the details in the preparation of clean diamond (001), the fact that it roughens at a very similar temperature to Si(001) supports our finding that surface energetics must play an important role here in the roughness, in light of the significantly stronger bond strength of diamond than silicon. In Ref. [10], the positive bias STM images of the edges at the upper terrace side of the S_B and D_B steps are considerably brighter than those of the S_A and D_A steps. This could be qualitatively understood from the structures in Figs. 1(b) and 1(d). In these two structures, the upper terrace edges consist of occupied and empty π orbitals; the π electrons are more loosely bounded compared with the σ electrons [24]; and the empty π orbitals are even less bounded. This leads to a large outward protrusion of the electronic states, most sensitive to the STM probe.

In summary, first-principles calculations reveal a completely different step physics of diamond (001) from that of silicon, despite that the physics of the flat surfaces, i.e., dimerization, are remarkably similar. A simple bond-counting rule is proposed, which can semiquantitatively account for the energy order of the various step structures and the roughness of the diamond (001). We expect that the rule may have a broader applicability to a whole range of sp^2-sp^3 hybrid systems such as nanodiamond [25], carbon foams [26], and other organic systems where different hybridizations coexist.

This work was supported by the National High Technology Development Program of China (No. 2002AA325090), the National Natural Science Foundation of China (No. 10634070, No. 10425418, No. 50672121), the National Basic Research (973) Program of China (No. 2007CB925000), and the Knowledge Innovation Project of Chinese Academy of Sciences. S. B. Z. was supported by the US DOE/BES and EERE under the Contract No. DE-AC36-99GO10337.

[1] *Handbook of Industrial Diamonds and Diamond Films*, edited by M. Prelas, G. Popovici, and L. Bigelow (Marcel Dekker, New York, 1998).
[2] J. C. Angus and C. C. Hayman, Science **241**, 913 (1988).
[3] T. P. Chow and R. Tyagi, IEEE Trans. Electron Devices **41**, 1481 (1994).
[4] P. Krüger and J. Pollmann, Phys. Rev. Lett. **74**, 1155 (1995).
[5] D. J. Chadi, Phys. Rev. Lett. **59**, 1691 (1987).
[6] A. A. Stekolnikovm, J. Furthmüller, and F. Bechstedt, Phys. Rev. B **68**, 205306 (2003).
[7] A. A. Stekolnikovm and F. Bechstedt, Phys. Rev. B **72**, 125326 (2005).
[8] M. D. Pashley, Phys. Rev. B **40**, 10481 (1989).
[9] L. Zhang, E. G. Wang, Q. K. Xue, S. B. Zhang, and Z. Zhang, Phys. Rev. Lett. **97**, 126103 (2006).
[10] K. Bobrov, A. J. Mayne, and G. Dujardin, Nature (London) **413**, 616 (2001).
[11] G. Kresse and J. Hafner, Phys. Rev. B **47**, 558 (1993).
[12] G. Kresse and J. Furthmüller, Phys. Rev. B **54**, 11169 (1996).
[13] G. Kresse and J. Furthmüller, Comput. Mater. Sci. **6**, 15 (1996).
[14] D. Vanderbilt, Phys. Rev. B **41**, 7892 (1990).
[15] Y. Wang and J. P. Perdew, Phys. Rev. B **44**, 13298 (1991).
[16] H. J. Monkhorst and J. D. Pack, Phys. Rev. B **13**, 5188 (1976).
[17] E. Pehlke and P. Kratzer, Phys. Rev. B **59**, 2790 (1999).
[18] F. A. Reboredo, S. B. Zhang, and Alex Zunger, Phys. Rev. B. **63**, 125316 (2001).
[19] P. Bogushawski, Q.-M. Zhang, Z. Zhang, and J. Bernholc, Phys. Rev. Lett. **72**, 3694 (1994).
[20] A. Oshiyama, Phys. Rev. Lett. **74**, 130 (1995).
[21] A. A. Stekolnikov, J. Furthmüller, and F. Bechstedt, Phys. Rev. B **65**, 115318 (2002).
[22] S. B. Zhang and A. Zunger, Phys. Rev. B **53**, 1343 (1996).
[23] R. J. Hamers, R. M. Tromp, and J. E. Demuth, Phys. Rev. B **34**, 5343 (1986).
[24] Y.-H. Kim, S. B. Zhang, Y. Yu, L. F. Xu, and C. Z. Gu, Phys. Rev. B **74**, 075329 (2006).
[25] J.-Y. Raty, G. Galli, C. Bostedt, T. W. van Buuren, and L. J. Terminello, Phys. Rev. Lett. **90**, 037401 (2003).
[26] H. R. Karfunkel and T. Dressler, J. Am. Chem. Soc. **114**, 2285 (1992).